Tissue characterization in cerebral ischemia using multiparameter MRI

Hamid Soltanian Zadeh[*a,b], Rabih Hammoud[a],
Michael A Jacobs[a,c], Suresh C Patel[a], Panayiotis D Mitsias[d],
Mamatha Pasnoor[d], Robert Knight[d], Zhang G. Zheng[d], Mei Lu[e], Michael Chopp[d]

[a]Department of Radiology, Henry Ford Health System, Detroit, MI 48202, USA

[b]Department of Electrical and Computer Engineering, University of Tehran, Tehran 14399, Iran

[c]Department of Radiology, John Hopkins University, Baltimore, MD 21205, USA

[d]Department of Neurology, Henry Ford Health System, Detroit, MI 48202, USA

[e]Department of Biostatistics, Henry Ford Health System, Detroit, MI 48202, USA

ABSTRACT

After pre-processing and segmentation, the proposed method scores tissue regions between 1 and N. Score 1 is assigned to normal white matter and score N to CSF. Lesion zones are assigned a score based on their relative levels of similarities to white matter and CSF. To evaluate the method, 15 rats were imaged by a 7T MRI system at one of the three time points (acute, sub-acute, chronic) after MCA occlusion. Then, they were sacrificed and their brains were sliced and prepared for histological studies. MRI of 2 or 3 slices of each rat brain, using 2 DWI (b = 400, b = 800), 1 PDWI, 1 T2WI, and 1 T1WI, was used and an MRI score between 1 and 100 (N = 100) was found for each region. Segmented regions were mapped onto the histology images and were scored by an experienced pathologist, from 1 to 10. MRI scores were validated using histology scores. To this end, correlation coefficients between the two scores (MRI and histology) were found. The results showed excellent correlations between MRI and histology scores at different time points.

Keywords: medical image analysis, tissue characterization, ISODATA, cerebral ischemia, stroke, magnetic resonance imaging, MRI

1. INTRODUCTION

The ultimate goal of medical imaging and analysis is to generate and extract important clinical information that would improve diagnosis and treatment of disease. In particular, accurate identification and discrimination of viable from necrotic tissue after stroke would enhance the management of patients. Magnetic resonance imaging (MRI) is highly sensitive to local changes in both tissue water and biophysical environment of tissue water. These environments can be probed using MR parameters, such as T1, T2, diffusion, and proton density, among others. Changes in tissue water reflect physiologic alterations that occur during the evolution of stroke and can be visualized by MRI. A sequence of MR images of the same anatomical site (an MR image set) contains information pertaining to the tissue parameters. This implicit information may be used for image analysis and tissue characterization.

Within an ischemic lesion, MR parameters are time dependent and heterogeneous and it is unlikely that a single MR parameter can characterize the complexity of cerebral tissue.[1–5] In clinical practice, diffusion, T2-, and T1-weighted images (DWI, T2WI, T1WI, respectively) are acquired during the progression of stroke at most medical centers. These MRI data provide complementary information about the status of the tissue. MRI generates multispectral or multiparametric data because of its unique ability to form images influenced by different types of tissue parameters (e.g., proton density, T2, T1, and diffusion).[6,7] By utilizing these MR images, an n-dimensional feature space can be constructed and unsupervised segmentation methods, such as K-means and fuzzy c-means can be applied for exploratory clustering and analysis.[8–10] A difficulty with K-means and fuzzy c-means segmentation methodologies is that the number of tissue clusters should be known a priori.[8,9] In practice, the number of tissue

* Correspondence: Emails: hamids@rad.hfh.edu, hszadeh@chamran.ut.ac.ir

clusters is not usually known during the evolution of cerebral ischemia, since the ischemic tissue damage is heterogeneous and time dependent.[3,4,11] These challenges require an algorithm that can adjust the number of tissue clusters in an iterative fashion and incorporate multiple MRI parameters.

To segment and characterize ischemic brain tissue damage independently of time, we have developed a computerized method using an iterative self organizing data analysis algorithm (ISODATA).[11,12] This method has advantages compared to the tissue signature model reported previously.[2,3] The tissue signature model was based upon the evolution of T2 and ADC during stroke. This supervised method required an operator to define a rectangular box on a scatter plot using the mean and standard deviation of normal tissue from T2 and apparent diffusion coefficient of water (ADC) maps.[2,13] The need for supervision to determine clusters was a limitation of the model. In contrast, the proposed unsupervised segmentation method is objective and requires no human interaction. It is an iterative, multi-step process, which assigns the input data into a set of clusters.

The proposed ISODATA method identifies clusters in the MRI feature space and partitions a brain image into normal and abnormal tissue regions using multiparametric MRI (e.g., T1-, T2-, PD-, and diffusion-weighted images). Segmentation results may be displayed as multiple binary images, one for each of the regions segmented, or as a single color-coded image. However, since the clusters are not always identified in the same order by ISODATA, the resulting segmentation results and the color-coded images, will have different cluster numbers and colors for similar tissue types, e.g., the normal tissues in different studies. To remedy this problem, we have devised a standardization method which takes the ISODATA results, orders the clusters, and generates consistent color-coded images.

The proposed method is validated using MRI and histological studies of rat brains. Multiparametric ISODATA measurements were obtained from different MRI data sets that consisted of combinations of DWI, T2, and T1. Multiparametric ISODATA measurements of the ischemic lesion were compared to the histological tissue correlates for efficacy of tissue identification and staging of the ischemic lesion at different time points after stroke. The working hypothesis tested in this study is that an integrated set of MR parameters can provide insight about the histological status of ischemic cerebral tissue.

The organization of the paper is as follows. The foundations and theoretical bases of the segmentation and characterization methods are reviewed in Section 2. Imaging procedures, image analysis steps, and evaluation methods are described in Section 3. Applications to rat brain studies are presented in Section 4. Conclusions are given in Section 5.

2. PROPOSED IMAGE ANALYSIS SYSTEM

A block diagram for the steps of the proposed method is given in Fig. 1. The very first step is image registration and warping which is explained next.

2.1. Image Registration and Warping

If the subject moves between different scans, images should be registered before multiparameter image analysis. We use the surface matching (head and hat) technique proposed by Pelizzari, Chen, and co-workers.[14] To get the contours, we use a multiresolution technique[15] to automatically extract the skin surface needed for the image registration algorithm.

To match the geometry of the diffusion weighted images acquired using fast imaging techniques with that of the conventional spin echo images (T1, T2, and PD-weighted), we apply the warping method developed by Ghanei, et al.[16]

2.2. Intracranial Volume Segmentation

Tomographic images consist of a representation of anatomical structures in a background. The image background does not usually contain any useful information but complicates the image analysis task and increases the processing time. It is therefore beneficial to remove the image background before any analysis begins. Also, for brain analysis, skull, scalp, eyes, and other structures that are outside the intracranial cavity are not of interest. We segment the intracranial cavity volume using a multiresolution technique.[15]

2.3. Noise Suppression

Noise limits the performance of both human observers and computer vision systems. As such, noise should be suppressed prior to inputing data to the image analysis algorithms. To reduce the computation time, the noise

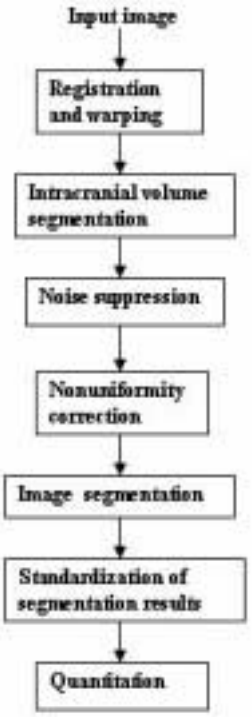

Figure 1. Flowchart of the image analysis system.

suppression is performed on the *intracranial* volume pixels only. We use a non-linear edge-preserving filter which has specifically been developed for MR image restoration.[17]

2.4. Non-Uniformity Correction

Ignoring the random noise, the measured MRI pixel gray level P_{ij} can be related to the true MRI signal by the relation $P_{ij} = A_{ij}I_{ij}$ where A_{ij} is the nonuniformity factor at location (i, j) in the image and I_{ij} is the artifact free intensity value at the same position. A number of approaches to the correction of radiofrequency (RF) induced intensity variations have been proposed.[18,19] All of these methods divide the acquired image by a reference image that approximates the nonuniformity profile A_{ij}, but differ in the way the reference images are obtained.

Considering the limitations associated with a uniform phantom, due to changing nonuniformity pattern over time and the coil's loading, we use the following approach which estimates the nonuniformity pattern from the acquired images. Assuming that the inhomogeneity in the RF coil sensitivity manifests itself as a low frequency component, we estimate A_{ij} by smoothing the image using a 33x33 kernel of 1's.[18] We have modified this approach by not averaging the background pixels to avoid the artifacts generated around the brain boundary. Also, in this modified version, to avoid edge artifacts, we replace pixel values in bright areas of the image, such as CSF in a T2-weighted image compared to other normal brain tissues, with the average gray level of the image.

2.5. Image Segmentation

Our approach to image segmentation is based on both of spatial and feature domain properties of the MRI data. The spatial domain properties include relationship between a pixel and its neighbors, e.g., connectivity with similar pixels (i.e., pixels with similar gray levels) or distance from the closest pixel with the same gray level. The

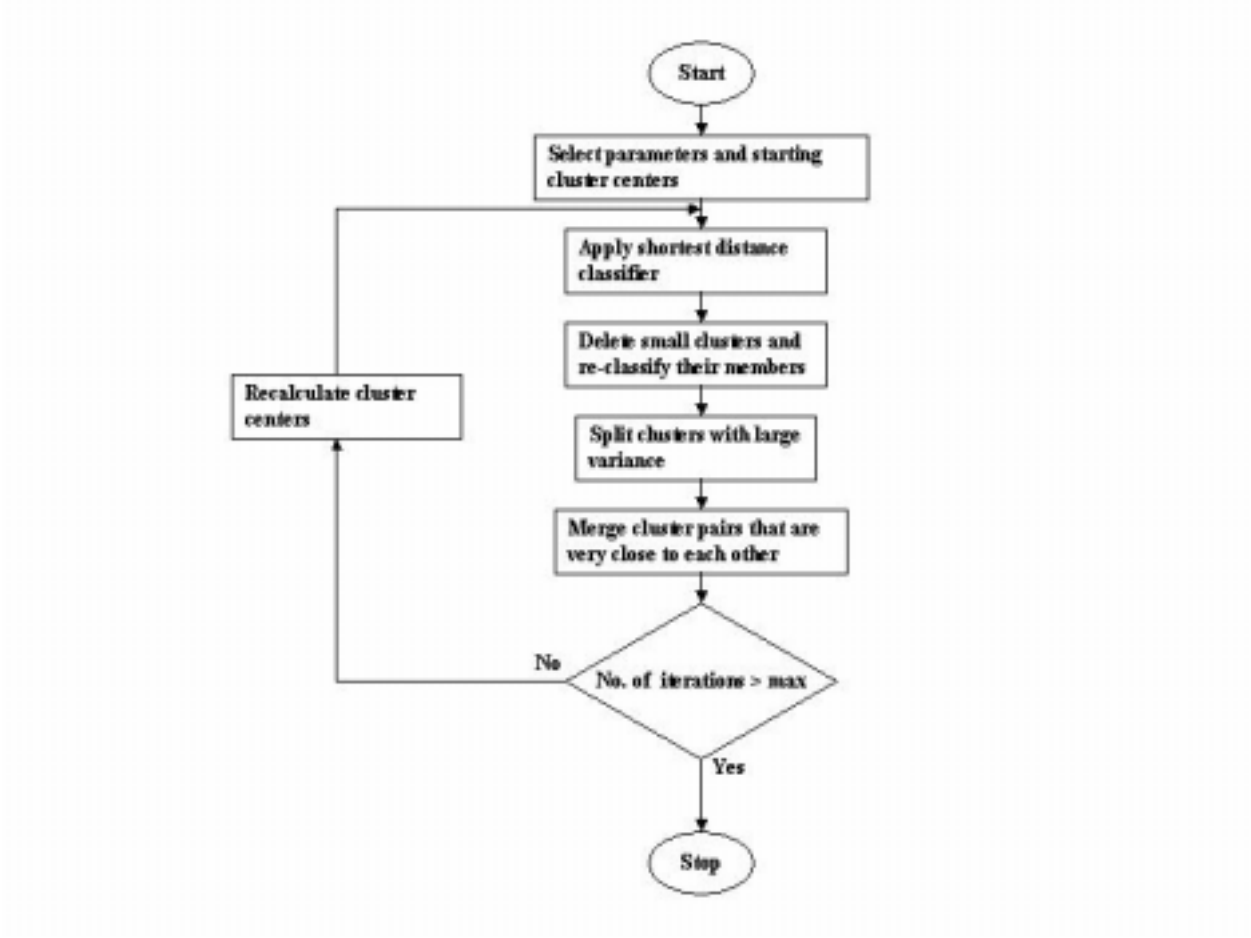

Figure 2. Flowchart of the image segmentation method.

feature domain properties include those of the image gray level distribution. We use a mode filter to extract spatial information and use a cluster analysis method to extract feature domain information from the MRI data.

We use an unsupervised clustering approach which is from the family of *Iterative Self Organizing Data Analysis Techniques* (ISODATA). The approach is similar in principle to the K-means clustering in the sense that cluster centers are iteratively determined sample means. However, it includes a set of additional merging and splitting procedures which have been incorporated into an interactive scheme. These steps have been incorporated into the algorithm as a result of experience gained through experimentation. A flowchart of the proposed approach is shown in Fig. 2. Details of the method are described in reference.[12]

2.6. Standardization of Segmentation Results

Utilizing the distribution of the tissue clusters in the MRI feature space, the above segmentation method yields a tissue signature vector (cluster center) for each cluster. If two clusters are close to each other in the feature space, then their coordinates will be similar and the Euclidean distance between the tissue signature vectors will be small. On the other hand, if the clusters are far apart in the feature space, this would imply that the measurements are different and the Euclidean distance will be large.

Within the context of cerebral ischemia, tissue that has undergone less severe ischemic damage will exhibit less histological damage and will have a low histological score (see below). We hypothesize that the MRI tissue signature for this tissue will have a small or no difference from that of the normal tissue. As the severity of ischemia increases, there is a corresponding increase in the histological damage to the tissue as indicated by both the Euclidean distance between tissue clusters in the MRI feature space and the histological scores.

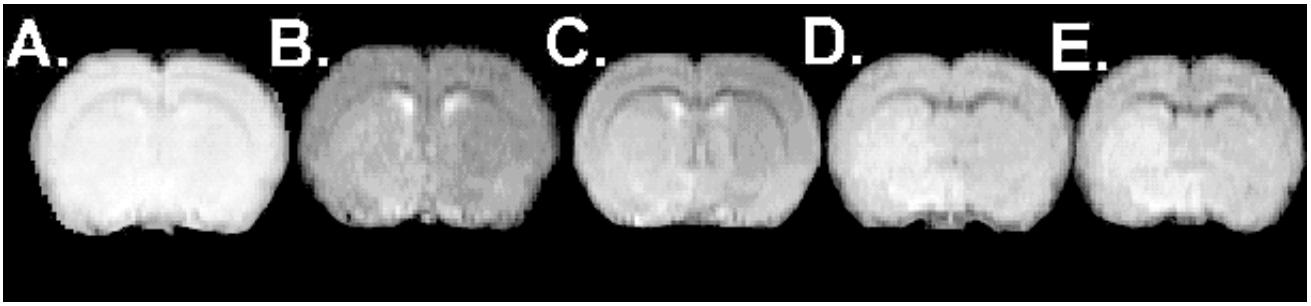

Figure 3. Representative acute (4-8 hr) MR images utilized in the proposed algorithm for rats subjected to experimental cerebral ischemia: A) Proton density (TE = 30 ms); B) T2-weighted (TE = 90 ms); C) T1-weighted image; D-E) Diffusion weighted images (D, b = 400 s/mm^2, E, b = 800 s/mm^2).

Here, the goal is to characterize the segmented tissues, i.e., score them in a range between r_1 and r_2, based on their MRI characteristics, so that r_1 represents normal brain and r_2 represents cavitated lesion (dead tissue) filled with CSF. To do this, we use the following equation to assign a score to each of the regions.

$$\text{MRI score} = \text{Integer part of}\Big[\frac{ED_{i1}}{ED_{i1} + ED_{i2}} \times (r_2 - r_1) + r_1\Big] \tag{1}$$

where ED_{i1} and ED_{i2} are the Euclidean distances between the signature vector (center) of the ith cluster and the signature vectors of the normal tissue and CSF, respectively. The numbers r_1 and r_2 are selected such that the final image has desirable colors. For example, they are selected to be 20 and 120 for the images shown in Fig. 5. The range $r_2 - r_1$ determines the resolution desired for tissue differentiation. Equation (1) assigns signature (score) r_1 to the normal brain matter and signature (score) r_2 to CSF. It assigns a score (signature number) to each of the lesion zones based on its levels of similarities (in terms of multiparametric MRI) to the normal brain matter and CSF.

3. VALIDATION STUDIES

3.1. Experimental Animal Model

All studies were performed in accordance with the institutional guidelines for animal research under a protocol approved by the Institutional Care of Experimental Animals Committee. Fifteen male Wistar rats weighing 270-310 g were subjected to permanent occlusion of the middle cerebral artery (MCA) occlusion by a method of intraluminal vascular occlusion.[20] Ischemic animals were classified based on sacrifice time after stroke: acute (4-8 hr, n = 5); subacute (16-24 hr, n = 7); chronic (48-168 hr, n = 3). Rats were anesthetized with 3.5% halothane, and maintained with 0.75-1.5% halothane in 70% N20 and 30% O2 using a face mask. Rectal temperature was controlled at 37^{o}C with a feedback-regulated water-heating pad. An incision (approximately 2 cm) was made at the midline of the neck and the right common carotid artery (CCA), external carotid artery (ECA), and internal carotid artery (ICA) were exposed. The bifurcation of the ECA and ICA was carefully dissected. The distal end of the ECA was ligated. The CCA and ICA were temporarily clamped using microvasculature clips. A small puncture was made in the ECA. Approximately 18.0-19.0 mm of 4-0 surgical nylon suture (with its tip rounded by heating near a flame) was inserted into the ECA and advanced into the ICA until it blocked the origin of the MCA. A 4-0 silk thread was then tightened around the suture and the microvasculature clips removed. This method produces a focal infarct in the striatum, i.e., caudate putamen and globus pallidus, that may extend into the cortex.[21]

3.2. MRI Studies

3.2.1. Image Acquisition

After MCA occlusion, the animal was placed in the magnet and MRI data sets (DWI, T2WI, and T1WI) were acquired on a 7T, 20 cm bore, superconducting magnet (Magnex Scientific Inc., Abingdon, U.K.) interfaced to a SMIS (Surrey Medical Imaging Systems Ltd., Guildford, U.K.) console. A 5 cm internal diameter birdcage radio frequency coil and 12 cm bore actively shielded gradient coil set capable of producing magnetic field gradients up to 20 gauss/cm were used. The head of the animal was secured using stereotaxic ear bars to reduce motion during the experiment. Once the animal is placed inside the magnet, two orthogonal interleaved fast low angle shot (FLASH)

images (coronal and sagittal planes) were acquired. Saturation effects at intersection of the two slice planes produce a dark band in each image indicating the axial position, angle, and thickness of the image slice through the brain. The FLASH images were acquired over a 5.0 cm field of view (FOV), 1 mm slice thickness and reconstructed using a 128x128 image matrix. The entire sequence required approximately one minute, allowing rapid, reproducible repositioning (within ±0.5 mm) of the animal in an iterative manner. The position of the animal is adjusted until the imaging slice is centered 5 mm posterior to the rhinal fissure with the head of the rat held in a flat skull position.

During MRI measurements, anesthesia was maintained with 0.5-1.0% halothane in a 70% N_2O and 30% O_2 gas mixture. Rectal temperature was monitored and controlled using a feedback-controlled water bath. MRI studies were performed on animals after MCA occlusion at acute, subacute, and chronic post ischemia time points. Multislice (2 mm thick slices) DWI, T2WI, T1WI were obtained using a 128x128 image matrix with a 32 mm FOV. DWI were acquired using the pulsed gradient spin-echo (PGSE) method described by LeBihan.[22] A two-dimensional Fourier transform (2DFT) PGSE was used with TR/TE = 1500/40 ms and diffusion weighted gradients (7 contiguous slices, with incremented b-values of 0, 200, 400, 600, and 800 s/mm^2, 2 NEX) applied along the z axis. T2WI were acquired using a multiecho sequence (7 contiguous slices, TR/TE = 3000 /30, 60, 90, and 120 ms, 1 NEX) and a T1-weighted inversion recovery image (5 contiguous slices, TR/TE = 6000/30 ms, TI = 750 ms, 1 NEX) was also obtained.

3.2.2. Image Analysis

All image analysis tasks were performed using a SUN UltraSparc2 workstation (Sun Microsystems Inc., Mountain View, CA). All MR images were reconstructed with a 128x128 matrix using in house software and subsequently processed using the Eigentool image analysis software.[23–26] Eigentool has a comprehensive set of functions for displaying, restoring, enhancing, and analyzing images. The complete toolbox consists of image analysis algorithms such as morphological operators, registration, and warping methods.[27]

After reconstruction, the image preprocessing steps described in Section 2 were applied. Preprocessed MRI was coregistered and warped to histology using a two step method.[27] The method consists of a modified head and hat surface-based registration algorithm that aligns the MRI to the histological section followed by nonlinear thin plate spline warping to compensate for distortions between the MRI and histological data sets. After coregistration and warping, the segmentation and standardization methods described in Section 2 were applied using two T2WI (TE = 30, 90 ms), T1WI, and two DWI (b = 400, 800 s/mm^2) images. Standardization was done using either white matter or gray matter as the normal brain matter, to investigate their impact on the results.

3.3. Histopathological Studies

3.3.1. Tissue Processing

All animals were sacrificed immediately after imaging for histopathological evaluation. Animals were deeply anesthetized with ketamine (44 mg/kg) and xylazine (13 mg/kg) by intraperitoneal injection and were transcardially perfused with heparinized saline and 10% neutral buffered formalin. The brain was removed and immersed in the same fixative overnight. Fourteen coronal blocks of brain tissue were cut at 1 mm intervals using a rat brain matrix. The tissue was processed and embedded in paraffin. Six micron (μm) thick paraffin sections from each block were cut and stained with hematoxylin and eosin (H&E) for evaluation of ischemic cell damage.

3.3.2. Regional Light Microscopy Analysis

The coregistered and warped MRI defined lesion areas were overlaid onto the corresponding H&E stained histological sections. From each segmented region, two to four fields of view (392x280 μm^2) in the ipsilateral hemisphere and the homologous areas in the contralateral hemisphere were digitized under a light microscope with a 40x objective lens (Olympus BX40) using a CCD camera (Hitachi RP-111, Tokyo, Japan) interfaced with Global Lab image analysis system (Data Translation, Marlboro, MA). Each image was analyzed with a MCID image analysis system (Research Imaging, St. Catherine's, Canada) and the coordinates for each image were recorded. A value of the mean gray scale of the entire image and two standard deviations of the mean was used to measure the number of cells and vacuolization. In addition, for measurement of vacuolization, we inverted images in order to obtain improved gray scale visualization. These values were selected based on our preliminary study in which we manually counted numbers of cells for each image and then compared the numbers of cells counted by the MCID image analysis system with several different thresholds of gray scale intensity within the same image. We compared the number of cells obtained from both manual and computer counting in more than 200 images utilizing the mean gray scale value from the entire image and two standard deviations. Differences in the numbers of cells between these two methods were less than 5%. In addition, two blinded observers (ZGZ, AVG) measured the number of cells in the same image (n =

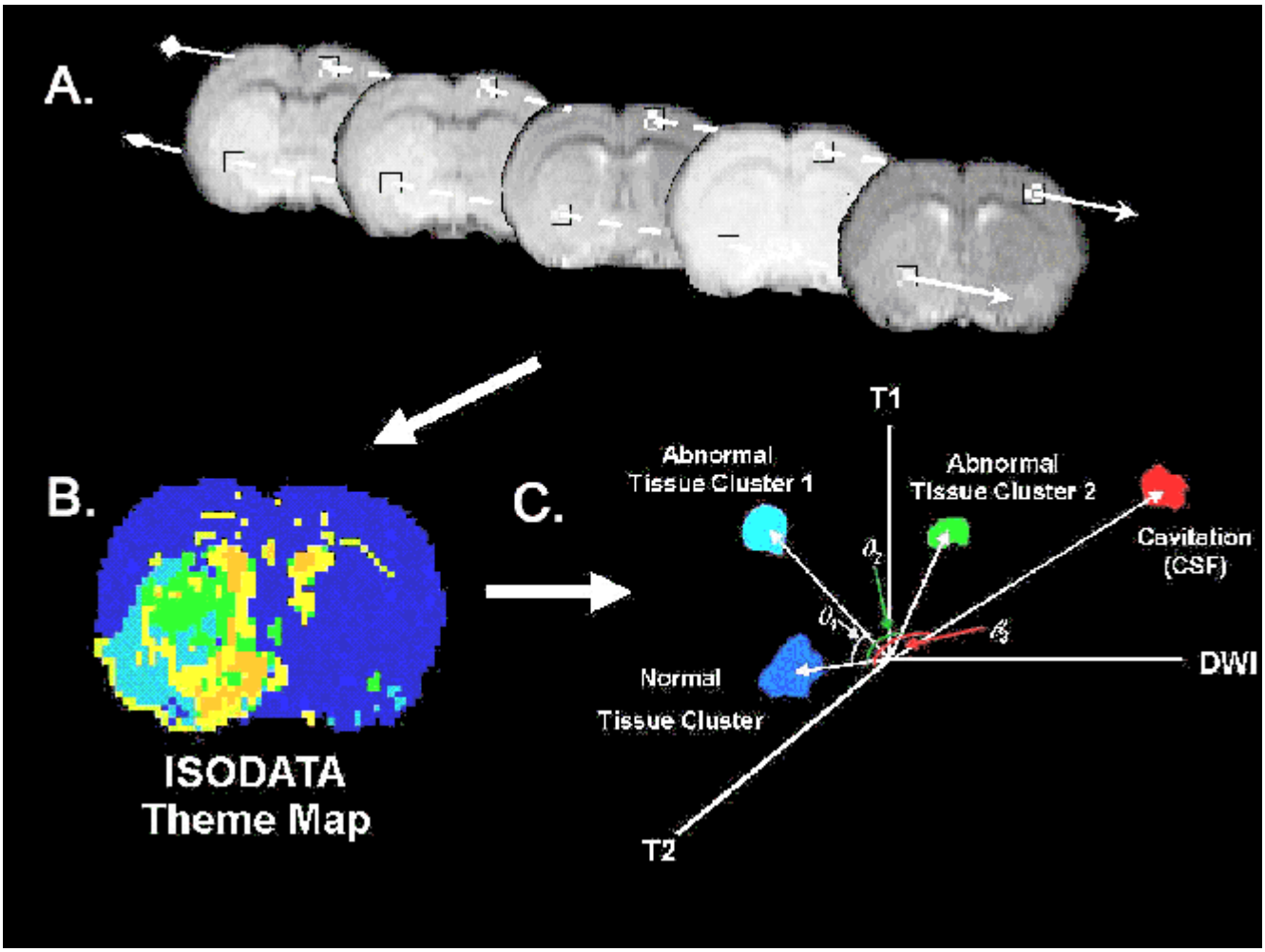

Figure 4. Illustration of tissue signature vectors for tissue types using MR images shown in Fig. 3. A) Tissue signature vectors used by ISODATA to segments tissues. B) An ISODATA image. The dark blue color encompassing the contralateral hemisphere and frontal and parietal cortex of the ipsilateral hemisphere represents normal tissue. The various colored regions (light blue to red) within the ipsilateral hemisphere represent abnormal tissues. CSF (red) is segmented as a separate tissue. C) A schematic of MRI feature space showing distribution of tissue clusters in 3D. Each axis represents signal intensity distribution of an MR image.

102) with these values and an interobserver difference of 1.25% was found. Changes in vacuolization were presented as a percentage of the field, in which, areas of vacuoles were divided by total field area.

3.3.3. Histological Grading

Based on prior studies in our laboratory,[21,28] the criterion for ischemic neuronal damage was the presence of scalloping at the cytoplasmic border, triangular shrunken neurons (acute ischemic neuronal damage), eosinophilic and ghost neurons (chronic ischemic damage). Because the MCID image analysis system could not differentiate these morphological changes, we combined numbers of cells quantified by the MCID image analysis system with visual observation of ischemic neuronal damage under the light microscope based on criteria outlined above. To reflect heterogeneous nature of the ischemic lesion evolution, we developed a grading scale ranging from 0-10 for the present study with no neuronal damage scored zero and the most severe neuronal damage scored ten. Neuronal shrinkage and morphological alterations were all considered potentially reversibly damaged tissue and scored as follows.

- 0 = no neuronal damage
- 1 = less than 20%

Table 1. Correlation Coefficients Between MRI Scores and Histology Scores and the Corresponding p Values in Parenthesis, using four different methods to determine MRI scores.

Time Point	Using WM	Using GM	Using WM and ROI	Using GM and ROI
Acute	0.86 (0.0003)	0.76 (0.0042)	0.90 (0.0008)	0.84 (0.0048)
Sub-acute	0.70 (0.0037)	0.57 (0.0250)	0.81 (0.0002)	0.67 (0.0058)
Chronic	0.59 (0.163)	0.80 (0.0321)	0.85 (0.0163)	0.92 (0.0035)
All Three	0.72 (< 0.0001)	0.73 (< 0.0001)	0.78 (< 0.0001)	0.72 (< 0.0001)

- 2 = between 21% and 50%
- 3 = greater than 50%
- 4,5 = combinations of 2 and 3, such that 1 is added to the score if less than 50% reduction in the number of total cells is seen as compared to the contralateral hemisphere or 2 is added for greater than 50% reduction in the number of total cells as compared to the contralateral hemisphere.

Neuronal necrosis, eosinophilia, red neurons, and ghost neurons were considered potentially irreversibly damaged tissue and scored as follows.

- 6 = less than 20%
- 7 = between 21% and 50%
- 8 = greater than 50%
- 9,10 = combinations of 7 and 8, such that, 1 is added to the score if less than 50% reduction in the number of total cells is seen as compared to the contralateral hemisphere or 2 is added for greater than 50% reduction in the number of total cells as compared to the contralateral hemisphere.

3.4. Statistical Analysis

We first evaluated normality of MRI and histology scores. If normality conditions were met, we calculated Pearson correlation coefficients using the the scores. Otherwise, we applied appropriate data transformation to the scores before calculating correlation coefficients, to make their distributions normal. Correlation coefficients between MRI and histology scores were calculated based on the slice information, assuming the independence between slices. We imputed the correlation coefficient using the images selected at individual time points and for all of the time points, with the calculation of p-value for testing of no correlation. A p-value smaller than 0.05 indicates a significant correlation between measurements compared to no correlation at all.

4. EXPERIMENTAL RESULTS

The proposed approach has been applied to MRI studies of rats with MCA occlusion and humans with cerebral ischemia. In this paper, we present the validation studies conducted using MRI and histological studies of rats. Representative MRI and segmentation and characterization results are shown in Figs. 3-5.

At three time points after MCA occlusion (acute, subacute, and chronic), two or three brain slices were selected from each rat and processed according to the above steps to segment and characterize tissue damage. In all studies, two DWI, two T2WI, and one T1WI were used and an MRI score between 1 and 100 was found for each tissue region. For each of the regions, a histology score was obtained from the histological study (see Fig. 6).

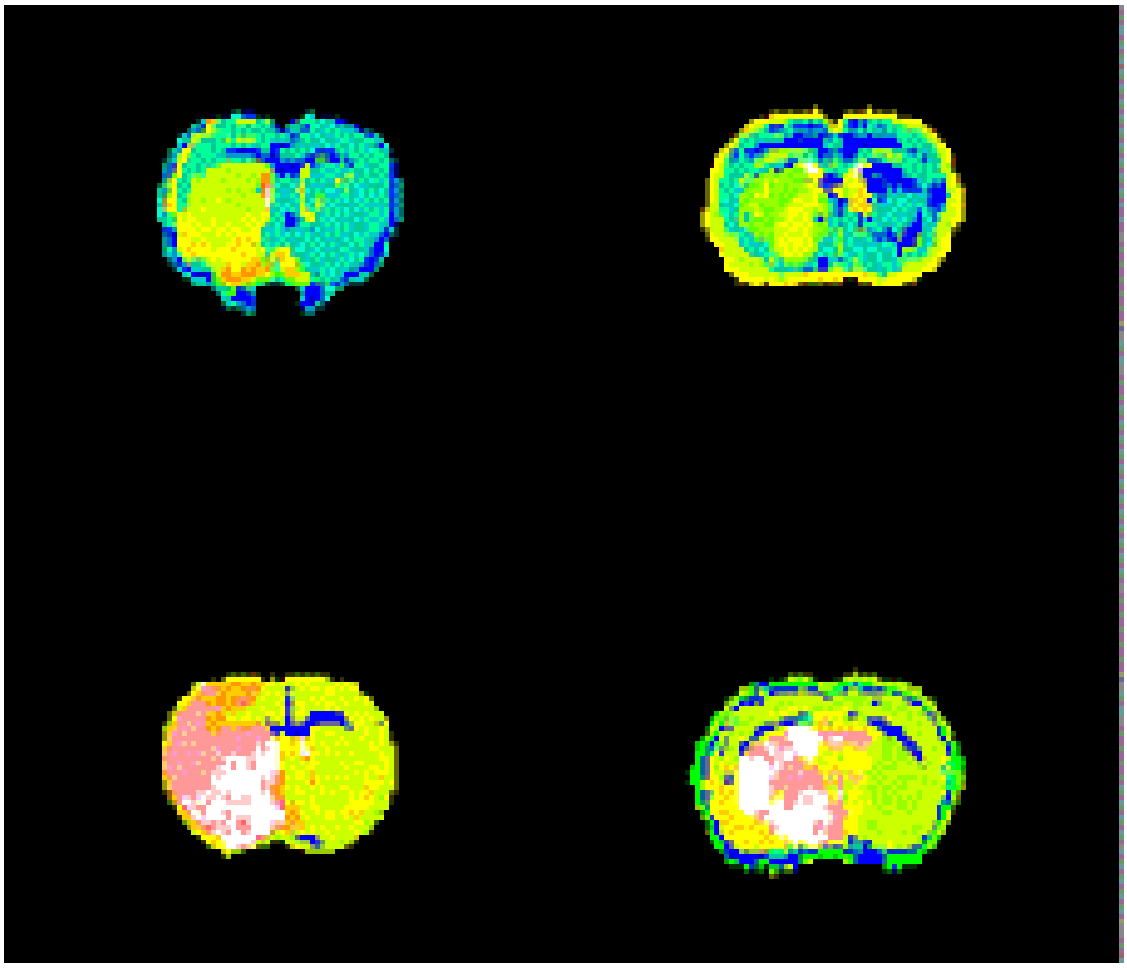

Figure 5. Standardized ISODATA images of four rat brains with MCA occlusion, showing different levels of tissue damage. The Euclidean distances (ED) between the normal tissue and abnormal tissue clusters, using tissue signature vectors, are utilized for standardization of the classified images and characterization of tissues over time. The greater the ED between abnormal and normal tissue clusters, the greater the histological damage. CSF or fluid filled cavitated regions is the endpoint for ischemic tissue.

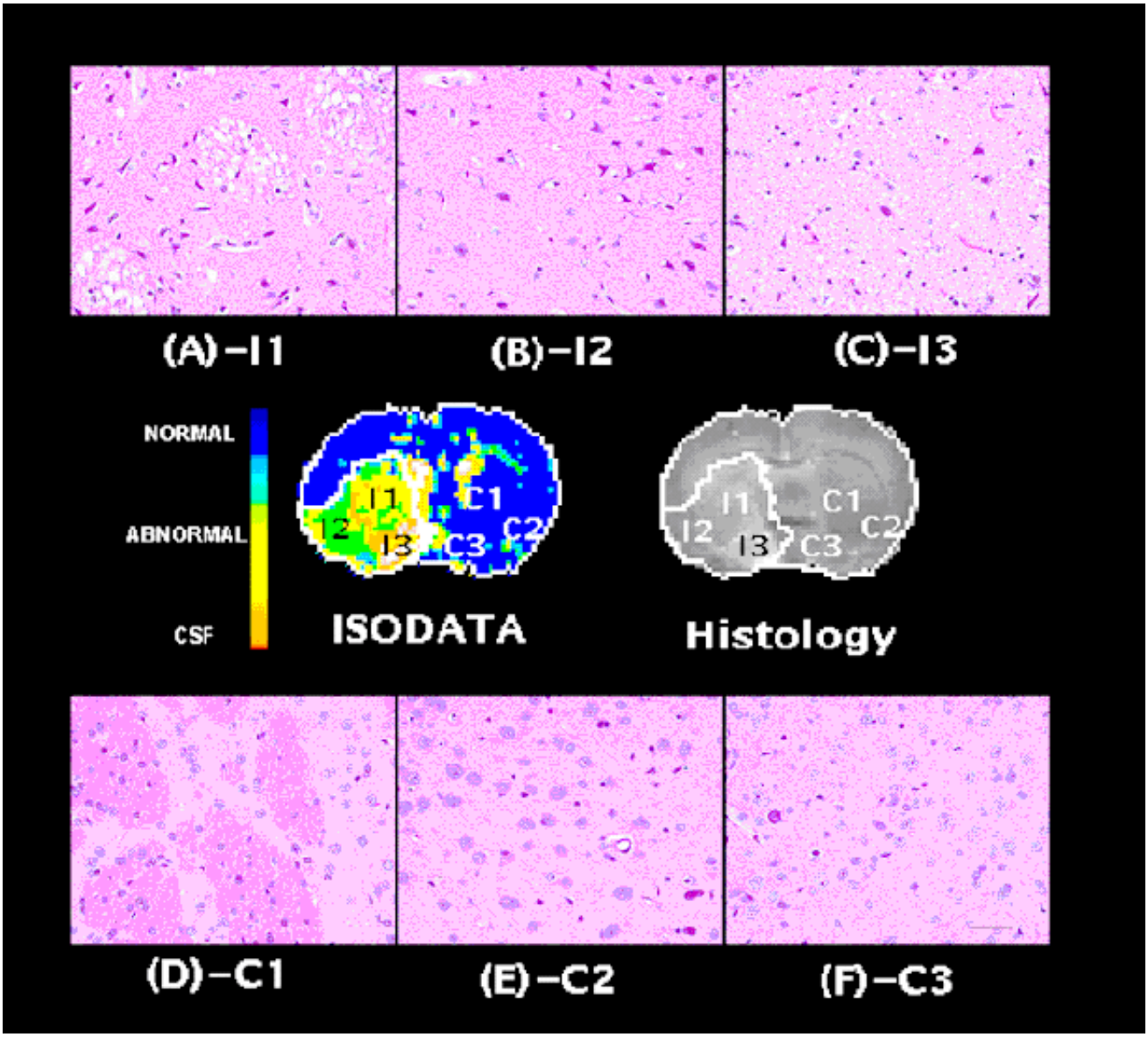

Figure 6. Warped ISODATA image from an acute (4-8 hr) animal after stroke, with lesion boundary overlaid onto the corresponding histological H&E stained section. A-F) Magnified regions (40x) taken from caudate putamen (I1, C1), periform cortex (I2, C2), and preoptic areas (I3, C3). A-C) Histological morphology within regions I1-I3 showing acute ischemic cellular damage. Histological changes are visualized as shrunken and triangular neuronal cell bodies with neuronal perikarya and surrounded by vacuoles (A, C). Tissue vacuolation corresponding to both swollen astrocytes and neurons is most prominent in striatum (I1, I3). D-F) Normal tissue within the contralateral regions C1-C3. Black bar scale is 50 μm long.

In these studies, two sets of standardized ISODATA images were generated; one using white matter (corpus callosum) as the normal brain matter and the second using gray matter as the normal brain matter. On each of the standardized ISODATA images, ROI's, corresponding to those used on the histology image to determine the histology scores, were drawn. MRI scores were determined for each of these ROI's using the standardization equation of Section 2.6. In addition, MRI scores were determined for the clusters on which these ROI's fell (see Fig. 6 and Table 1).

Relationship of the MRI scores, obtained using the above methods, to the histology scores were explored. To this end, the correlation coefficients between the two scores (MRI and histology) and the corresponding p-values were found for each time point and for all of the time points (acute, sub-acute, and chronic).

Thirty-four MRI slices from 15 rats were processed and scored. The corresponding histology scores were also obtained. Twelve of the MRI's were at the acute time in 5 rats, another 15 of the MRI's were at the sub-acute time in 7 rats, and 7 of the remaining MRI's were at the chronic time in 3 rats. Correlation coefficients and the corresponding p-values, presented in Table 1, illustrate excellent correlations between MRI and histology scores at different time points.

5. CONCLUSIONS

The proposed method segments normal and abnormal brain tissues and characterizes (accurately scores) tissue damage in cerebral ischemia based on multiparameter MRI data. The method is useful for a variety of applications in the field of computer aided diagnosis and treatment including response to treatment. For example, volume changes for different zones of the lesion over time (e.g., tissue recovery) can be evaluated.

The method is promising for distinguishing abnormal tissues from normal tissues and different abnormalities from each other. It can serve as a tissue characterization tool in MRI. It may help radiologists achieve more accurate diagnoses and let therapists and surgeons deliver more effective treatments to the patients.

ACKNOWLEDGMENT

This work was supported in part by NINDS grant PO1 NS-23393 and NSF grant BES-9911084.

REFERENCES

1. Fisher M, Prichard JW, Warach S. New magnetic resonance techniques for acute ischemic stroke. Jama 1995;274:908-911.
2. Jiang Q, Chopp M, Zhang Z, Knight R, Jacobs M, Windham J, Peck D, Ewing J, Welch K. The temporal evolution of MRI tissue signatures after transient middle cerebral artery occlusion in rat. J Neurol Sci 1997;145:15-23.
3. Welch K, Windham J, Knight RA, Nagesh V, Hugg JW, Jacobs M, Peck D, Booker P, Dereski M, Levine S. A model to predict the histopathology of human stroke using diffusion and T2-weighted magnetic resonance imaging. Stroke 1995;26:1983-1989.
4. Knight R, Dereski M, Helpern J, Ordidge R, Chopp M. Magnetic resonance imaging assessment of evolving focal cerebral ischemia: comparison with histopathology in rats. Stroke 1994;25:1252-1262.
5. Baird A, Warach S. Magnetic resonance imaging of acute stroke. J Cere Blood Flow Metab 1998;18:583-609.
6. Vannier MW, Butterfield RL, Rickman DL, Jordan DM, Murphy WA, Biondetti PR. Multispectral magnetic resonance image analysis. Radiology 1985;154:221-224.
7. Vannier MW, Pilgram TK, Speidel CM, Neumann LR, Rickman DL, Schertz LD. Validation of magnetic resonance imaging (MRI) multispectral tissue classification. Computerized Medical Imaging and Graphics 1991;15:217-23.
8. Clarke LP, Velthuizen RP, Camacho MA, Heine JJ, Vaidyanathan M, Hall LO, Thatcher RW, Silbiger ML. MRI segmentation: methods and applications. Magnetic Resonance Imaging 1995;13:343-68.
9. Zijdenbos A, Dawant B. Brain segmentation and white matter lesion detection in MRI images. Crit Rev Biomed Eng 1994;22:401-465.
10. Jain A, Dubes R. Algorthims for clustering data. New York: Prentice Hall Advanced Reference Series, 1988.
11. Jacobs MA, Knight R, Soltanian-Zadeh H, Zheng Z, Goussev A, Peck D, Windham J, Chopp M. Unsupervised segmentation of multiparameter MRI in experimental cerebral ischemia with comparison to T2, Diffusion, and ADC MRI parameters and histopathological validation. J Magn Reson Imaging 2000;11:425-437.

12. Soltanian-Zadeh H, Windham J, Robbins L. Semi-supervised segmentation of MRI stroke studies. Proc SPIE 1997;3034:437-448.
13. Jacobs MA, Windham J, Knight R, Welch K, Peck D, Jiang Q, Chopp M. Methodology for MRI characterization of tissue histopathology during the evolution of cerebral ischemia in rat using feature space representation. J Cere Blood Flow Metab 1995;15 (Suppl 1):S125.
14. Pelizzari CA, Chen GTY, Spelbring DR, Weichselbaum RR, Chen CT. Accurate three-dimensional registration of CT, PET and MR images of the brain. J Comput Assist Tomogr 1989;13(1):20-26.
15. Soltanian-Zadeh H, Windham JP. A multi-resolution approach for intracranial volume segmentation from brain images. Medical Physics 1997; 24(12):1844-1853.
16. Ghanei A, Soltanian-Zadeh H, Jacobs M, Patel S. Boundary-based Warping of Brain MR Images. Journal of Magnetic Resonance Imaging 2000;12(3):417-429.
17. Soltanian-Zadeh H, Windham JP, and Yagle AE. Magnetic resonance image restoration using a new multi-dimensional non-linear edge-preserving filter. IEEE Trans Imag Proc 1995;4(2):147-161.
18. Lim KO, Pfefferbaum A. Segmentation of MR brain image into cerebrospinal fluid spaces and white and gray matter. J Comput Assist Tomogr 1989;13:588-593.
19. Dawant BM, Zijdenbos AP, Margolin RA. Correction of intensity variation in MR images for computer-assisted tissue classification. IEEE Trans Med Imag 1993;12(4):770-781.
20. Zea Longa, Weinstein P, Carlson S, Cummins R. Reversible middle cerebral artery occlusion without craniectomy in rats. Stroke 1989.;20:84-91.
21. Zhang R, Chopp M, Chen H, Garcia J. Temporal profile of ischemic tissue damage, neutrophil response, and vascular plugging following permanent and transient (2H) middle cerebral artery occlusion in the rat. J Neuro Sci 1994;125:3-10.
22. Le Bihan D, Breton E, Lallemand D, Grenier P, Cabanis E, Laval Jeantet M. MR imaging of intravoxel incoherent motions: application to diffusion and perfusion in neurologic disorders. Radiology 1986;161:401-407.
23. Windham JP, Abd-Allah MA, Reimann DA, Froelich JW, Haggar AM. Eigenimage filtering in MR imaging. J Comput Assist Tomogr 1988;12:1-9.
24. Soltanian-Zadeh H, Windham J, Peck D, Yagle A. A comparative analysis of several transformations for enhancement and segmentation of magnetic resonance image scene sequence. IEEE Trans Med Imaging 1992;11:302-318.
25. Peck D, Windham J, Emery L, Soltanian-Zadeh H, Hearshen D, Mikkelsen T. Cerebral tumor volume calculations using planimetric and eigenimage analysis. Med. Phys. 1996;23:2035-2042.
26. Jacobs MA, Knight R, Windham J, Zheng Z, Soltanian-Zadeh H, Goussev A, Peck D, Chopp M. Identification of cerebral ischemic lesions in rat using eigenimage filtered MRI. Brain Res. 1999;1-2:83-94.
27. Jacobs MA, Windham J, Soltanian-Zadeh H, Peck D, Knight R. Registration and warping of magnetic resonance images to histological sections. Med Phys 1999;26:1568-1578.
28. Garcia J, Yoshida Y, Chen H, Li Y, Zhang Z, Lian J, Chen S, Chopp M. Progression from ischemic injury to infarct following middle cerebral artery occlusion in the rat. Am J Pathol 1993;142:623-635.